



UNIVERSITY OF LEEDS

This is a repository copy of *Internal twist drill coolant channel modelling using computational fluid dynamics*.

White Rose Research Online URL for this paper:
<http://eprints.whiterose.ac.uk/89798/>

Version: Accepted Version

Proceedings Paper:

Johns, AS, Hewson, RW, Merson, E et al. (2 more authors) (2014) Internal twist drill coolant channel modelling using computational fluid dynamics. In: Oñate, E, Oliver, J and Huerta, A, (eds.) Proceedings, vol. II. 11th World Congress on Computational Mechanics (WCCM), 5th European Conference on Computational Mechanics (ECCM), 6th European Conference on Computational Fluid Dynamics (ECFD), 20-25 Jul 2014, Barcelona, Spain. International Center for Numerical Methods in Engineering (CIMNE) , pp. 1114-1122. ISBN 978-84-942844-7-2

Reuse

Unless indicated otherwise, fulltext items are protected by copyright with all rights reserved. The copyright exception in section 29 of the Copyright, Designs and Patents Act 1988 allows the making of a single copy solely for the purpose of non-commercial research or private study within the limits of fair dealing. The publisher or other rights-holder may allow further reproduction and re-use of this version - refer to the White Rose Research Online record for this item. Where records identify the publisher as the copyright holder, users can verify any specific terms of use on the publisher's website.

Takedown

If you consider content in White Rose Research Online to be in breach of UK law, please notify us by emailing eprints@whiterose.ac.uk including the URL of the record and the reason for the withdrawal request.



eprints@whiterose.ac.uk
<https://eprints.whiterose.ac.uk/>

INTERNAL TWIST DRILL COOLANT CHANNEL MODELLING USING COMPUTATIONAL FLUID DYNAMICS

AS. JOHNS*, RW. HEWSON[†], E. MERSON[‡], JL. SUMMERS* AND HM.
THOMPSON*

* School of Mechanical Engineering
University of Leeds, UK.
e-mail: sc07aj@leeds.ac.uk.

[†] Department of Aeronautics
Imperial College London, UK.
e-mail: r.hewson@imperial.ac.uk.

[‡] Sandvik Coromant
Sheffield, UK.
e-mail: eleanor.merson@sandvik.com

Key words: Computational Fluid Dynamics, Twist-Drills, Helical Flows, OpenFOAM

Abstract. Coolant technologies have become increasingly used within twist-drill machining. Internal helical coolant channels are a common means of delivering high-pressure coolant directly to the cutting edge to increase the transfer of heat away from the cutting edge and to aid with chip evacuation. However, the complex behaviour of Coriolis and centrifugal forces generated by large angular velocities and the curvature of the coiled channel govern the highly turbulent flow of coolant. This research uses Computational Fluid Dynamics (CFD) to study the design of internal coolant channels across the internal section of the drill bit.

1 INTRODUCTION

Since the first report of cutting fluids in 1894 by F. Taylor [1], the use of cutting fluids within the twist-drill machining of metals has increased. Internal helical coolant channels are a common method of applying coolant directly to the cutting edge, main source of heat from the drilling process, without having the delivery of coolant obstructed by chips exiting the cutting zone. The use of this coolant technology has been shown to increase tool life by lowering the operating temperature of cutting tools, improving average surface finish [2] and has also been observed to aid chip evacuation which prevents tool breakage

[3].

The complex influence of Coriolis and centrifugal forces generated by large angular velocities (up to 14,000rpm) and the curvature of the coiled channel have a significant impact on the highly turbulent flow of this coolant. Furthermore, the free surface flow, chip generation and transportation and heat transfer located at the cutting zone makes this a particularly complex problem. Due to limitations in experimental methods there is a limited understanding of cutting fluid behaviour in the the transport of heat and cuttings away from the cutting zone. In light of these limitations, a numerical approach has been adopted using Computational Fluid Dynamics (OpenFOAM, www.openfoam.org) to understand and improve the delivery of coolant to the cutting zone.

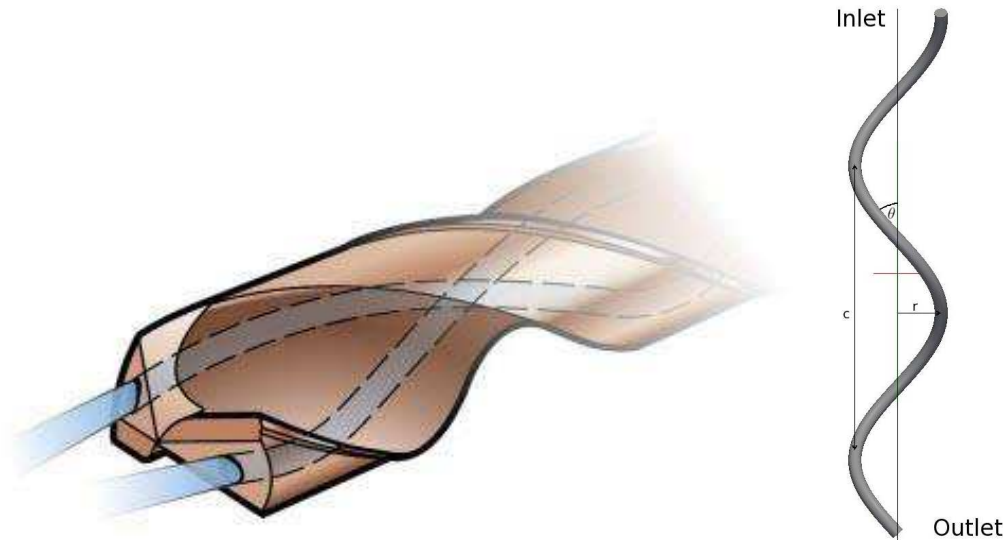


Figure 1: (Left) Example drill geometry containing helical coolant channels [4]. (Right) Illustration of helical coolant channel.

2 MATHEMATICAL MODEL

2.1 GOVERNING EQUATIONS

The through-tool flow of coolant is assumed to be single phase, isoviscous and isothermal as heat is localised at the cutting edge. Steady-state incompressible Navier-Stokes equations are solved for Newtonian flow, using finite volume discretisation. The solver uses the SIMPLE algorithm for pressure-velocity coupling. Rotation is accounted for by solving the momentum equation for relative velocity, \mathbf{U}_r , and including Coriolis forces as source terms, this implies that there is no mesh movement for the rotation of the drill.

The formulation of the Navier-Stokes equations in the rotating frame of reference is

$$\nabla \cdot \mathbf{u}_r = 0 \quad (1)$$

$$\nabla \cdot (\mathbf{u}_r \otimes \mathbf{u}_r) + 2\boldsymbol{\Omega} \times \mathbf{u}_r + \boldsymbol{\Omega} \times \boldsymbol{\Omega} \times \mathbf{r} = -\nabla \left(\frac{p}{\rho} \right) + \nu \nabla \cdot \nabla (\mathbf{u}_r) \quad (2)$$

Where pressure is p , density ρ , viscosity ν , $\boldsymbol{\Omega}$ is the speed of rotation in rad/s and \mathbf{r} is the radial position vector from the centre of rotation. Dirichlet boundary conditions are prescribed for velocity at the inlet and for outlet pressure and no-slip conditions are set for the walls, from this the pressure drop across the internal coolant channel was then calculated.

Preliminary experiments performed at a Sandvik Coromant facility calculated an average velocity of 80m/s for 40mm drills and 60m/s for 120mm drills with a radius 0.5mm using water. This data was used for inlet velocity boundary conditions within numerical calculations. With corresponding Reynolds (Re) numbers between $30,000 \leq 80,000$, Dean (Dn) numbers within the range of $1000 \leq 3000$ and Rossby (Ro) numbers above 20,000. These dimensionless numbers are defined as

$$\begin{aligned} Re &= \frac{\rho U L}{\mu} \\ Dn &= Re \left(\frac{L}{2D} \right)^{\frac{1}{2}} \\ Ro &= \frac{U}{LF} \end{aligned} \quad (3)$$

where μ liquid viscosity, U the average velocity, L is the length scale, F is the angular velocity and D the helix diameter. The large Reynolds number suggests the flow is turbulent; this was accounted for by using a standard k-epsilon turbulence model with wall-functions. The large Rossby number implies that rotation will not have a significant effect on the flow of coolant and the large Dean number implies large centrifugal forces caused by channel curvature. This analysis suggests that centrifugal forces will have the dominant effect over Coriolis forces due to the axial velocity of the fluid being considerably larger than the speed of rotation

2.2 MESH GENERATION

A structured straight pipe mesh was initially created with arc length defined parallel to the z axis. The centre-line of a helix with helix radius r and pitch θ is constructed using the equations

$$\begin{aligned} x(t) &= r \sin(t) \\ y(t) &= r \cos(t) \end{aligned} \quad (4)$$

$$z(t) = ct$$

Where r , c and θ are illustrated in Figure 1 and are the radius of the helix, distance between coils and pitch respectively. θ is defined as

$$\theta = \sin^{-1} \left(\frac{4r}{c} \right) \quad (5)$$

The channel radius is accounted for by scaling the cross section of the straight pipe during transformation, for this work coolant channels with a radius of 0.5mm are examined. When transforming the pipe into a helix, the z coordinate of the straight pipe identifies the point's position along the arc length and maps the arc length of the straight pipe to the corresponding helical centre-point position, $\mathbf{R}(s)$, in addition to the $\mathbf{T}(s)$, $\mathbf{N}(s)$ and $\mathbf{B}(s)$, which are the tangent, normal and bi-normal unit vectors at $\mathbf{R}(s)$. These are defined using the Frenet Serret formula as shown in Figure 2 and equations 6

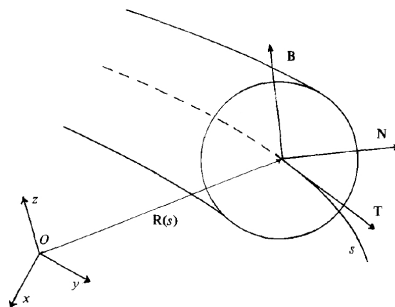


Figure 2: Illustration of the Frenet Serret Formula [5]

$$\begin{aligned} \mathbf{T} &= \frac{d\mathbf{R}}{ds} \\ \mathbf{N} &= \frac{1}{\kappa} \frac{d\mathbf{T}}{ds} \\ \mathbf{B} &= \mathbf{T} \times \mathbf{N}. \\ \frac{d\mathbf{N}}{ds} &= \tau\mathbf{B} - \kappa\mathbf{T} \\ \frac{d\mathbf{B}}{ds} &= -\tau\mathbf{N} \end{aligned} \quad (6)$$

where κ is the curvature and τ the torsion. The transformation is performed by translating points by the appropriate centre point of the helix before rotating by the $\mathbf{N}(s)$ and $\mathbf{B}(s)$

unit vectors to correct the inclination of the cross section. The resulting transformation can be seen in Figure 1 and is expressed formally as

$$\mathbf{H}(s) = \mathbf{R}(s) + P_x(s)\mathbf{N}(s) + P_y(s)\mathbf{B}(s) \tag{7}$$

Here $H(s)$ is the transformed position of any point along the arc length s , $P_x(s)$ and $P_y(s)$ are the cross sectional x and y coordinates respectively of any point along the straight pipe at arc length s .

3 MESH SENSITIVITY ANALYSIS

In order to ensure all flow features are accurately captured a mesh sensitivity study was performed. As a result of adopting a transformation approach when representing the geometry of coolant channels, resolution is not defined relative to global Cartesian coordinates. Mesh resolution is defined relative to the helix arc length and across the diameter of each channel cross section. Here, arc length resolution represents the number of cross sections used to represent the channel. The effects of mesh resolution were studied by examining the change in predicted pressure drop as a function of arc length resolution and cross section resolution for an extreme case of 60° pitch, drill length 40mm and radial spacing of 3.3mm. These results are shown in Figure 3. (Left) examines the change in

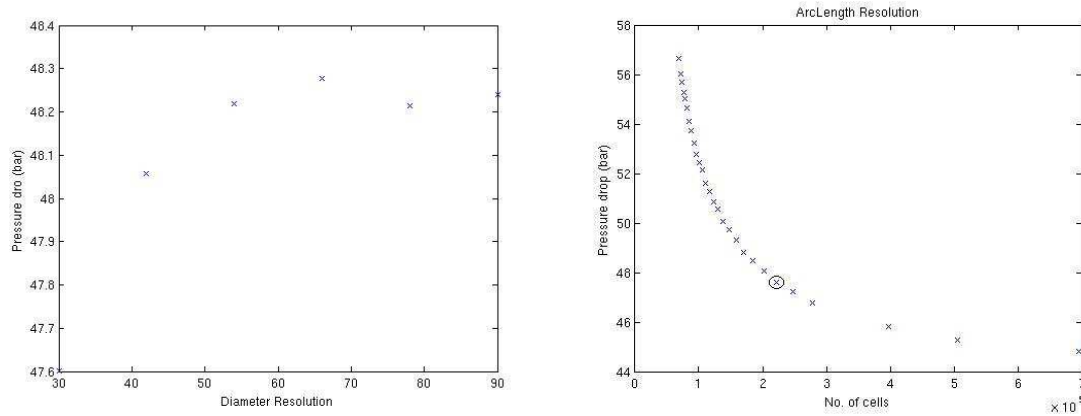


Figure 3: Mesh sensitivity study, the change in predicted pressure drop when changing (Left) cross section resolution across the diameter and (Right) arc length resolution.

calculated pressure drop as the number of cells across the diameter of each cross section varies. Current mesh refinement was found reasonable as the pressure drop fluctuated by less than 2% when increasing resolution. (Right) displays the total number of cells against the predicted pressure drop, cross section resolution is constant and arc length resolution is iteratively increased. The circled point was chosen for the model because predicted pressure drop varies by less than 5% when further increasing the number of cells by a factor of 2.

4 FRICTION FACTOR ANALYSIS

CFD predictions of pressure drop are validated against friction factor correlations derived from stationary helical flows due to general lack of experimental data encompassing rotating helical flows. Guo [6] experimentally investigated the frictional pressure drop for stationary helical flows at Reynolds numbers up to 150,000. Friction factors were calculated for stationary helical flow simulations using the same expression

$$p = \frac{f_c n \pi R \rho u^2}{4 r 2} \quad (8)$$

Here f_c is the friction factor for curved pipes, n is the number of coil loops and u the mass velocity in m/s. Figure 4 shows our present predictions in comparison with the friction factors predicted using Guo's [6] correlations. Our friction factor coefficients show good agreement with Guo's friction factor correlation [6], our calculated friction factors are within 20%, despite using channels ten times smaller in diameter.

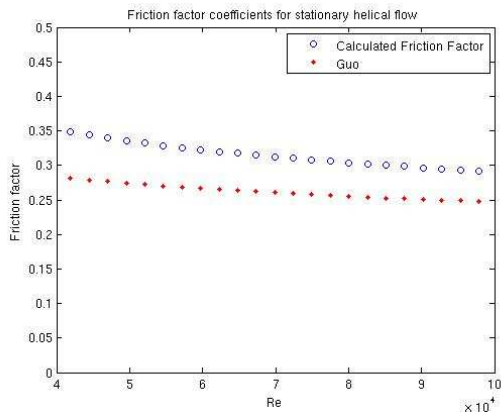


Figure 4: Comparison of friction factor coefficients, our model \circ (numerical), Guo \diamond [6] (empirical).

5 EFFECTS OF ROTATION

The effects of co-rotation and counter rotation on the flow structure within helical channels have been thoroughly researched by Yamamoto [7]. Co-rotation is where the helix rotates in the direction of axial flow and counter-rotation is rotation in the opposite direction of axial flow. Yamamoto's numerical modelling of rotating helical channels found that the centrifugal and Coriolis secondary flow forces operate in an additive sense for co-rotation, strengthening the secondary flow. However for counter-rotation, the Coriolis forces are shown to compete against the centrifugal forces.

In the application of twist-drill machining, the problem is bound to co-rotation due to

the geometry of the cutting tool. Numerical tests were carried out for a fixed geometry with pitch 30° , channel diameter of 1mm, helix radius of 3.3mm and an unconstrained speed of rotation $0 \leq 10,000\text{rpm}$. Figure 5 displays pressure drop as a function of speed of rotation in rpm; as the speed of rotation increases the pressure drop increases at a very small and constant rate. As suggested by large Rossby numbers in Section 2.1, it is clear that rotation has little effect on the flow of high pressure coolant through small twist drills, as can be seen by the difference in pressure drop between 0 and 10,000rpm being less than 1%. However pressure drop is not completely independent of rotation and in order for rotation to take a more significant effect on the flow of coolants, channels either need to be positioned further from the centre of rotation or the supply of coolant needs to be reduced.

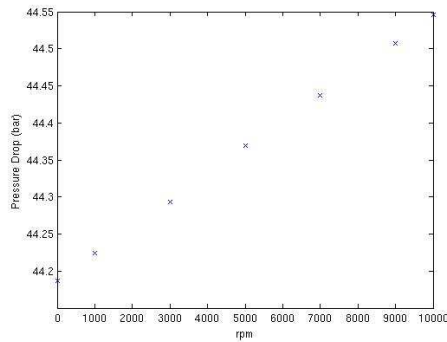


Figure 5: CFD pressure drop calculation as a function of speed of rotation

6 SECONDARY FLOW

Research by Yamamoto [7, 8, 9, 10, 11, 12] and Zhang [13] provide insight into the secondary flow behaviour of fluids through rotating helices. Figure 6 compares contours of the axial flow calculated by Yamamoto for co-rotating helices. However, their research numerically studies helices of different curvature and torsion at much smaller Dean numbers, although the size, shape and number of cells will be different for this research a similar axial motion is to be expected. As demonstrated in Figure 6, our model mirrors velocity contours seen in previous helical flow studies and therefore realistically models the velocity profile through rotating helices.

7 DISCUSSION

A CFD model for steady state flow through internal coolant channels has been constructed within this research which shows to have agreement with a number of previous works encompassing helical flows and internal coolant channels. Agreement with Guo's friction factor correlation [6] has been found. The effects of curvature observed in Hüttl's

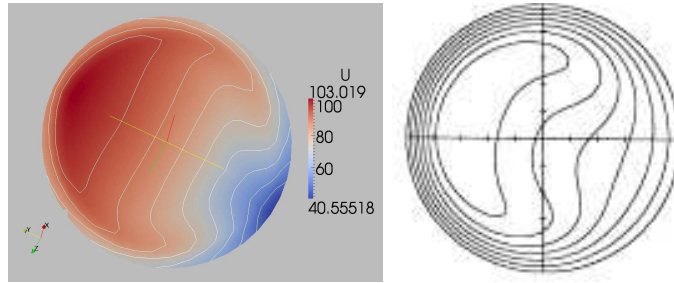


Figure 6: (Left) Axial helical velocity contour from our model. (Right) Axial velocity contour calculated by Yamamoto [7]

work on helical channels [14, 15] are also reproduced in this study. Typical helical flow behaviour described by Yamamoto [7] and Zhang [13] has also been reproduced. Finally, drill coolant channel flow has been shown to have a small dependence on angular velocity, which is in agreement with the Rossby number. Multiphase modelling will be the focus of future work to gain an understanding of what happens in the cutting zone under realistic operating conditions. This research would enable the analysis of the effects of channel size, shape and positioning on the direction of coolant at the channel exit and identify areas of the tool which require additional cutting fluids.

REFERENCES

- [1] Avila, R. and Abrao, A. The effect of cutting fluids on the machining of hardened aisi 4340 steel. *Journal of Materials Processing Technology*, vol. 119, 1 (2001) 21–26.
- [2] Haan, D., Batzer, S., Olson, W., and Sutherland, J. An experimental study of cutting fluid effects in drilling. *Journal of Materials Processing Technology*, vol. 71, 2 (1997) 305–313.
- [3] Braga, D.U., Diniz, A.E., Miranda, G., and Coppini, N. Using a minimum quantity of lubricant (mql) and a diamond coated tool in the drilling of aluminum–silicon alloys. *Journal of Materials Processing Technology*, vol. 122, 1 (2002) 127–138.
- [4] Coromant, S. Coolant knowledge base. <http://www.sandvik.coromant.com> (2013).
- [5] Germano, M. On the effect of torsion on a helical pipe flow. *Journal of Fluid Mechanics*, vol. 125, 1 (1982) 1–8.
- [6] Guo, L., Feng, Z., and Chen, X. An experimental investigation of the frictional pressure drop of steam–water two-phase flow in helical coils. *International journal of heat and mass transfer*, vol. 44, 14 (2001) 2601–2610.

- [7] Yamamoto, K., Alam, M., Yasuhara, J., and Aribowo, A. Flow through a rotating helical pipe with circular cross-section. *International Journal of Heat and Fluid Flow*, vol. 21, 2 (2000) 213 – 220.
- [8] Yamamoto, K., Aribowo, A., Hayamizu, Y., Hirose, T., and Kawahara, K. Visualization of the flow in a helical pipe. *Fluid Dynamics Research*, vol. 30, 4 (2002) 251–267.
- [9] Yamamoto, K., Yanase, S., and Jiang, R. Stability of the flow in a helical tube. *Fluid Dynamics Research*, vol. 22, 3 (1998) 153 – 170.
- [10] Yamamoto, K., Yanase, S., and Yoshida, T. Torsion effect on the flow in a helical pipe. *Fluid Dynamics Research*, vol. 14, 5 (1994) 259 – 273.
- [11] Alam, M., Ota, M., Ferdows, M., Islamv, M., Wahiduzzaman, M., and Yamamoto, K. Flow through a rotating helical pipe with a wide range of the dean number. *Archives of Mechanics*, vol. 59, 6 (2007) 501–517.
- [12] Yamamoto, K., Akita, T., Ikeuchi, H., and Kita, Y. Experimental study of the flow in a helical circular tube. *Fluid Dynamics Research*, vol. 16, 4 (1995) 237–249.
- [13] Zhang, J. and Zhang, B. Dean equations extended to a rotating helical pipe flow. *Journal of engineering mechanics*, vol. 129, 7 (2003) 823–829.
- [14] Hüttl, T. and Friedrich, R. Influence of curvature and torsion on turbulent flow in helically coiled pipes. *International Journal of Heat and Fluid Flow*, vol. 21, 3 (2000) 345–353.
- [15] Hüttl, T. and Friedrich, R. Direct numerical simulation of turbulent flows in curved and helically coiled pipes. *Computers & fluids*, vol. 30, 5 (2001) 591–605.